Magnetic diagnostics for plasmas

Contents

BASIC EQUATIONS

The electromotance or voltage ε ($-\varepsilon = \mathbf{E}$, the electric field intensity) in Volts induced in a circuit equals the rate of change of flux N in Wbs^{-1}:

$$\varepsilon = \frac{dN}{dt}$$

i.e.

$$\oint_l \mathbf{E}\ \mathbf{dl} = -\frac{d}{dt}\oint_S \mathbf{B}\ \mathbf{n} dS$$

for any path l, with n the normal to a two sided surface S.

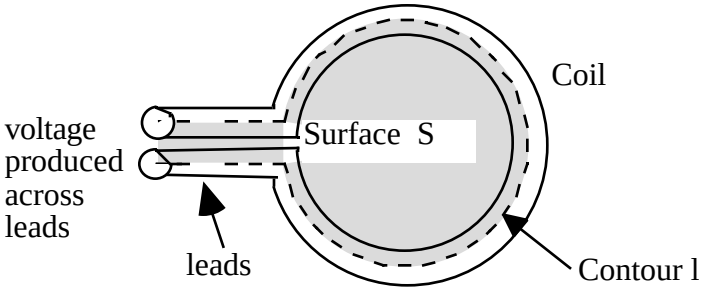

Figure. The contour l and surface S of a pick-up coil.

To obtain the required B the coil output signal must be integrated. This is performed passively with a resistance-capacitance circuit, with active integrators, or numerically on a computer after digitizing the data.

Integration

The time integration required to obtain the magnetic field B from the pick-up coil output ε can be performed either digitally or by an analog circuit.

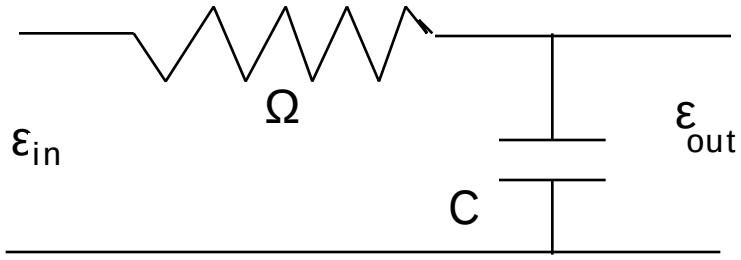

Figure. A passive "ΩC" integration circuit.

The simplest thing to do is to use a capacitor (C) and resistor (Ω) network, as shown in *Figure.* The output voltage is given by

$$\frac{d\varepsilon_{out}}{dt} + \frac{\varepsilon_{out}}{\tau} = \frac{\varepsilon_{in}}{\tau}$$

with $\tau = \Omega C$ called the integrator time constant. The solution to this equation is

$$\varepsilon_{out} = e^{-t/\tau}\int_0^t \left(e^{-t'/\tau}\,\varepsilon_{in}(t')\right)\frac{dt'}{\tau}$$

For example, suppose at t = 0 we start an input voltage $\varepsilon_{in} = \varepsilon_{in0}\sin(\omega t)$, so that the required integral is $\varepsilon_{int} = \varepsilon_{in0}\,(1-\cos(\omega t))/\omega$. The output from the passive circuit is (obtained using Laplace transforms)

$$\varepsilon_{out} = \varepsilon_{in0}\left(\frac{\omega\tau}{e^{t/\tau}\left(1+(\omega\tau)^2\right)} + \frac{\sin(\omega t) - \omega\tau\cos(\omega t)}{\left(1+(\omega\tau)^2\right)}\right)$$

Now consider two extremes. First, if $\omega\tau >> 1$ and $t << \tau$ we have

$$\varepsilon_{out} = \frac{\varepsilon_{in0}}{\omega\tau}\left(1-\cos(\omega t)\right)$$

That is, ε_{out} = $1/\tau$ times the required integral. In this limit we have integrated the input signal. If $\omega\tau << 1$ and $t >> \tau$, then $\varepsilon_{out} = \varepsilon_{in}$.

As an example, we show in *Figure* the output from the passive integrator ("integrator output", dotted line) for a sinusoidal voltage input of 1V at a frequency of 100 Hz ("coil input", solid line), with an integrator time $\tau = 0.1$s. The exact integral ("field") divided by τ is shown as the broken line. The integral is only performed accurately for times $t << \tau$; as the pulse proceeds there is a "droop", and significant errors result. We can imagine the curve "field" represents a specified magnetic field time history $B = B_0(1-\cos(\omega t))/(\omega\tau)$, with $B_0 = \tau/(nA)$ T, and B/τ is plotted. The curve "coil output" represents the non-integrated output from a magnetic pick-up coil with area nA m^2, (n turns each of area A), which becomes the input voltage to a passive integrator $\varepsilon_{in} = \sin(\omega t)$. Finally the curve "integrator output" represents the output from the passive integrator, which we would interpret as the original magnetic field.

A common situation is that the required signal from the pick-up coil has a low frequency component of angular frequency ω_0, and superimposed upon this is a higher frequency unwanted "noise" signal of angular frequency ω_1. By carefully choosing the time constant τ of our passive integrator so that $\omega_0\tau << 1$ ($\varepsilon_{out} = \varepsilon_{in}$) but $\omega_1\tau >> 1$ (integration) we filter the noise, leaving the required slowly time varying voltage. As an example, Figure shows the passive integrator output ε_{out} (dashed line) for an input voltage ε_{in} (solid line) comprising a slow ($\omega_0 = 10$ rs^{-1}, $\varepsilon_{in0} = 1$ V) and fast ($\omega_1 = 2x10^3$ rs^{-1}, $\varepsilon_{in1} = 0.2$ V) component. The time constant $\tau = 0.01$ s, so that $\omega_0\tau = 0.1$ ($<< 1$) and $\omega_1\tau = 100$ ($>> 1$). The output voltage is filtered, as required. The dashed line shows the exact integral divided by τ, for comparison.

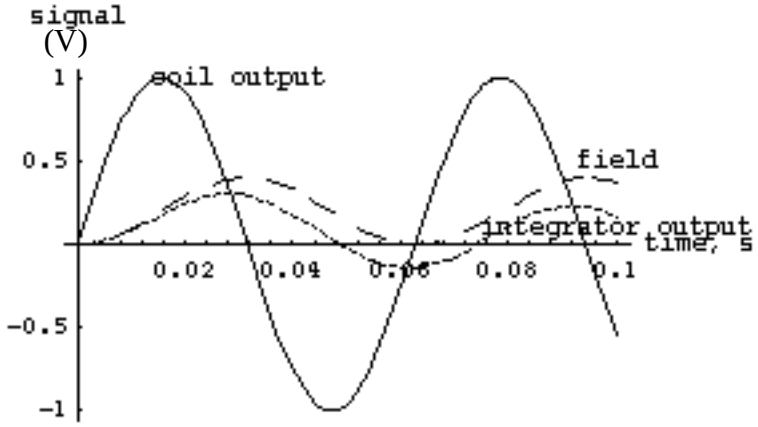

Figure. The input ("coil input", solid line) sinusoidal voltage with f = 100 Hz and output ("integrator output", dotted line) of a passive integrator circuit with $\tau = \Omega C = 0.1$ s. The (exact integral)/τ is denoted by "field", the broken line.

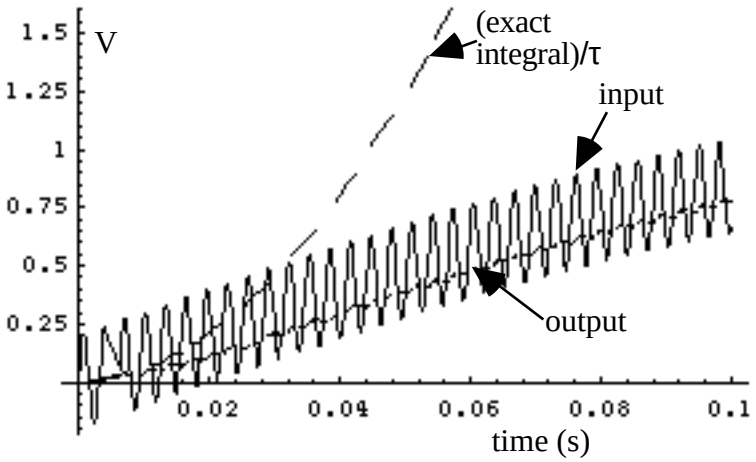

Figure The output of a passive integrator circuit used as a filter. An input voltage (solid line) with summed sinusoidal voltages is smoothed to give the dash-dot line. The exact integral divided by $\tau = \Omega C$ is shown as the dashed line.

A more common system to perform the time integration is an active integrator, but in many cases an input filter consisting of a passive integrator is still used. Active integration is performed using a circuit such as shown in *Figure*; the output voltage $\varepsilon_{out} = \frac{1}{\Omega C}\int_{t_1}^{t} \varepsilon_{in} dt$. The example shown grounds one side of the coil. A useful feature shown is the integrator gate, which defines the time t_1 the integration starts. On tokamaks this gate is often used to help reduce errors from misaligned pick-up coils. For example, tokamaks have a large toroidal field and a much smaller poloidal field. Therefore if the pick-up coil used to measure the poloidal field is misaligned even by a small amount, the resulting component of the toroidal field which is picked up (as dB/dt) can be significant. However the toroidal field usually evolves on a much slower time scale than the poloidal field, and in fact it is usually time independent at the time the poloidal field is initiated. Therefore the integrator gate can be opened when the toroidal field is time independent, and therefore the induced voltage in the misaligned pick-up coil is independent of the toroidal field.

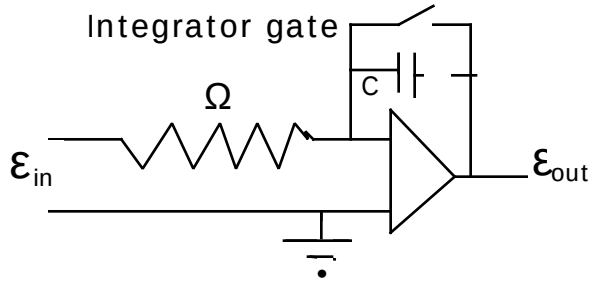

Figure. An active integrator circuit.

If the data is digitized, integration can be performed numerically. Sufficiently fast systems now exist for "real time" integration; the integration can be performed in μs so that integrated signals

suitable for real time feedback control can be obtained. A p bit digitizer has a resolution of 1 part in 10^p, e.g. an 8 bit system has a resolution of 1 in 256, while a 10 bit system has a resolution of 1 part in 1024. This can be a limitation if we intend to investigate large but low frequency magnetic fields in the presence of small, high frequency fields. An example is that of trying to measure the equilibrium poloidal field in the presence of Mirnov oscillations. The pick-up coil output is dominated by the voltage produced by the time derivative of the small but high frequency component. Avoiding saturating the input by the higher voltage, high frequency component means that the resolution of the low frequency fields is now restricted. If we want to use the full capability of the digitizer in recording the lower frequency fields, then the solution is to filter the signal and only allow frequencies below a certain value to be recorded, i.e. use the analog filters described above.

Intuition suggests that if a time varying wave form is sampled sufficiently fast then the original wave form can be recovered. However, we must determine how close the samples must be, and how to interpolate between adjacent points. The sampling theorem provides answers to these questions. An original signal x(t) can be recovered from sample values $x(nt_s)$, with t_s the sample time, by locating sinc functions at nt_s with amplitudes $x(nt_s)$. The signal x(t) can only be recovered if the signal bandwidth $b \leq f_s/2$, with f_s the sampling frequency = $1/t_s$. If this is not done, aliasing occurs.

If $b > f_s/2$ then the high frequency signal can appear as a low frequency signal. The fact that spoked wheels in films sometimes appear to rotate backwards is a manifestation of aliasing. Aliasing can be avoided using a passive filter to remove the high frequencies $f > f_s/2$. For example, sampling at 5 kHz (i.e. a sample every 0.2 ms) then an “anti aliasing” filter with $\tau = 0.5$ ms can be used.

ALTERNATE MEASUREMENT TECHNIQUES

Other techniques (than pick-up coils) are used to measure magnetic fields. The most common alternative is a Hall probe, shown in *Figure* A semiconductor is placed in a field B, and a current I driven perpendicular to B. The current carriers experience a Lorentz force, producing a charge build up in the direction perpendicular to both B and I. The resulting charge build up produces an electric field which cancels the magnetic force. This electric field is measured by electrodes. Discovered in 1879 in Johns Hopkin University.

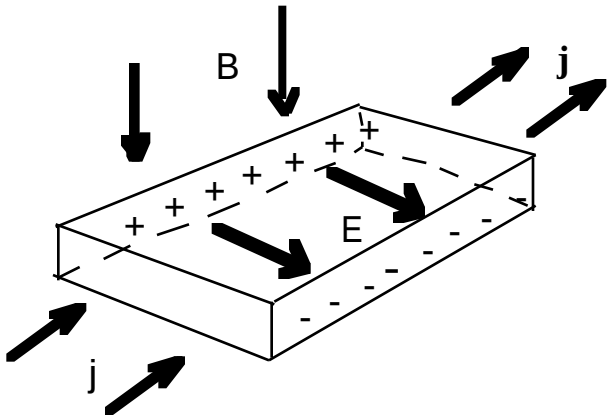

Drive j. Charge build up perpendicular to B and j. Measure E.

Figure. A Hall probe.

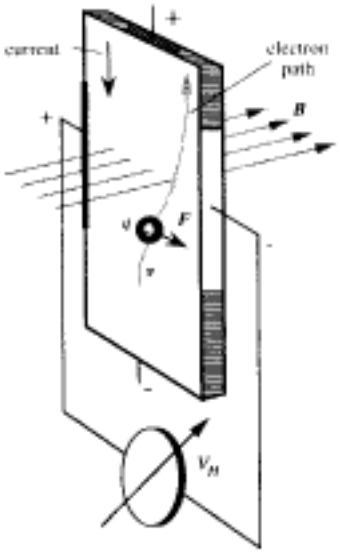

Assume electrons move inside flat conductive strip in B field. Then

$$V_H = hiB\sin(\alpha)$$

i is current, h is efficiency which depends on geometry, temperature, area. Theoretically the overall efficiency depends on the Hall coefficient, the transverse electric potential gradient per unit B field per unit current density.

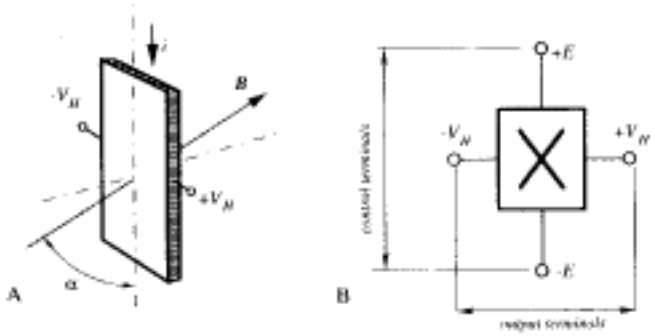

Problems: susceptibility to mechanical stress, and temperature (of resistors).

Faraday Effect

It has also been proposed to use the magneto-optic effect (the Faraday effect) in fused silica single mode optical fibers to measure magnetic fields, and the electro-optic (Kerr) effect to measure electric fields. The Faraday effect is the consequence of circular birefringence caused by a longitudinal magnetic field. Circular birefringence causes a rotation F of the plane of linearly polarized light, given by

$$F = V_c \oint_l \mathbf{H} \cdot d\mathbf{l}$$

around a contour l. No time integration is required. The Verdet constant $V_C \approx 5x10^{-6}$ radA^{-1} for silica. Thus the rotation must be now measured.

Another approach is to coat a fiber with magnetostrictive material and measure the strain effects, with the fiber as one arm of a Mach Zender interferometer.

The Compass.

Chinese 2634 BC, magnetite suspended on silk.

Flux gates

Intended for weak fields. See B-H curve below.

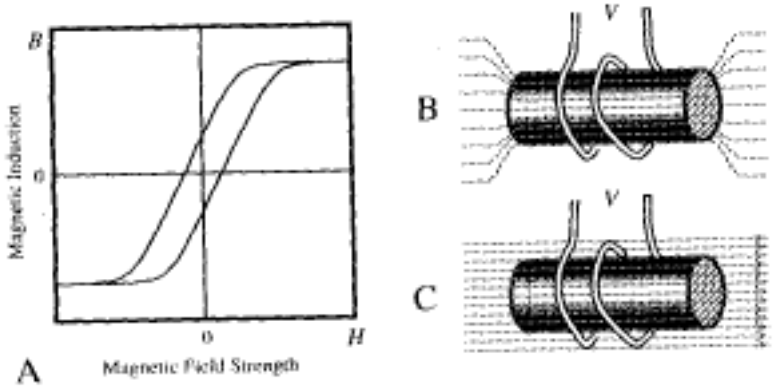

An applied field H to the core induces a magnetic flux B = mH. For high B the material saturates and μ is very small. There is hysterisis, and the path is different for increasing and decreasing H. When the core is not saturated the core acts as a low impedance path to lines of magnetic flux in the surrounding space. When the core is saturated the magnetic field lines are no more affected by the core. Each time the core passes from saturated to unsaturated and backwards, there is a change to the magnetic field lines. A pickup coil around the core will generate a spike. Flux lines drawn out of core implies positive spike, lines drawn into core, a negative spike. Amplitude of spike proportional to intensity of flux vector parallel to the sensing coil. Pulse polarity gives direction.

Core must be driven in and out of saturation by a second coil. The excitation current will induce a corresponding current in the sensor coil, but this can be allowed for.

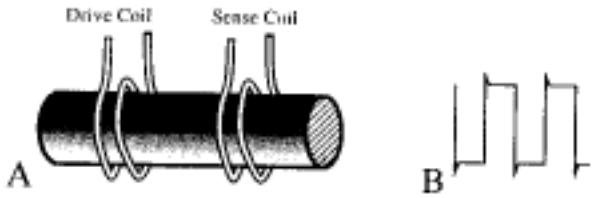

A better approach: position excitation coil so that it will excite without affecting sensor coil. i.e. excite flux at right angles to axis of sensor coil. Use toroidal core with drive winding and a cylindrical sensor coil..

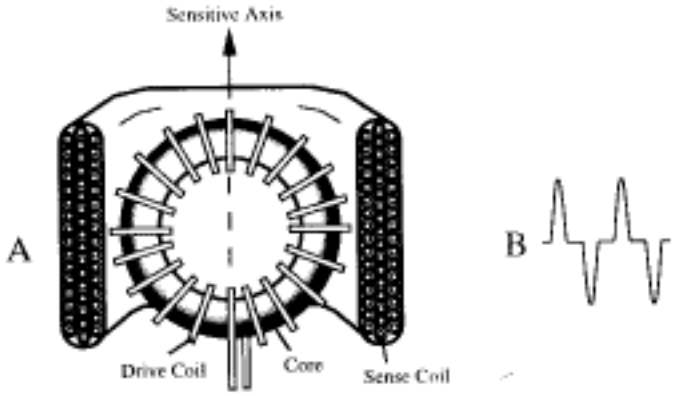

EXPERIMENTAL TECHNIQUES

Coils winding

The rogowski coil is simply made by obtaining a delay cable, and returning the wire down the center of the delay line (to ensure no net single turn is left). More complicated coils must be made by using variable winding densities (i.e. changing the pitch) or varying the cross sectional area of the former on which the coil is wound.

Interference suppression

Electrical equipment designed to produced RF energy such as generators, and switching phenomena in electrical circuits, create RF spectra which must be contended with.

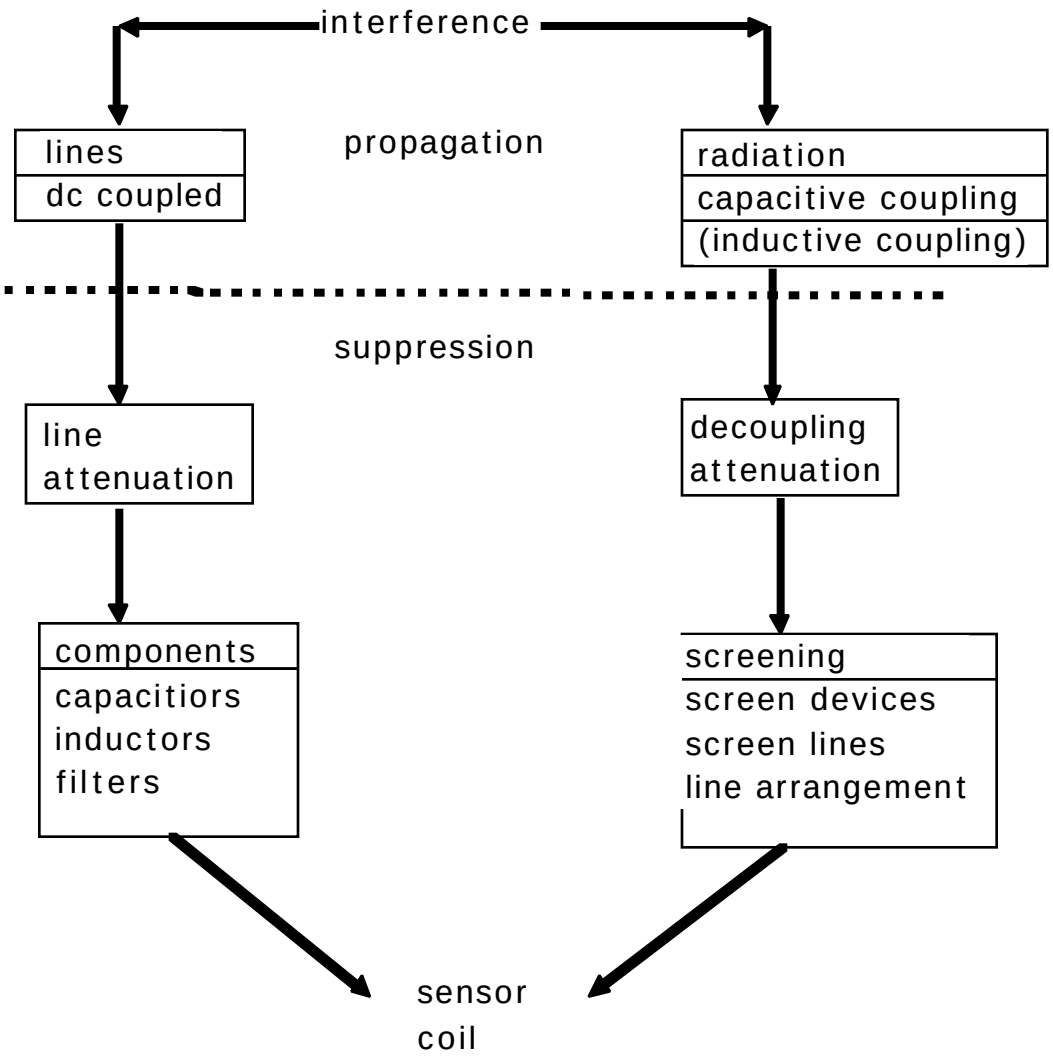

Figure. An illustration of interference paths and suppression techniques.

The sources of interference are illustrated in *Figure.* The interference propagates either down lines (cables) or by direct radiation. If the wavelength is large compared to the dimensions of the interference source only minor radiation will result, which is mostly found along the lines. This is the case for frequencies up to 30 MHz. When the dimension of the interference source is about that of the wavelength the interference energy will travel by radiation. The dominant frequencies are those where the interference source are l/4 or multiples of it. Favorable radiation conditions imply reduced line propagation (because of increased line attenuation) . Therefore the two propagation paths, comprising direct and capacitive or inductive coupling, suggest two means of suppression, either line attenuation or de-coupling attenuation. Line attenuation is effected by filters. De-coupling attenuation is effected by the construction of the sensor coil and the associated connecting lines.

A common problem with probes is capacitive pick-up. To test for this pick up on simple sensor coils, two identical and adjacent coils can be connected in series. Depending on the orientation, the signal obtained should be twice that measured with a single coil, or zero. If the coils connected in opposition do not give a zero signal, then capacitive coupling effects should be considered as a possible source of error. Capacitive coupling can be over using a grounded screen or can around the sensor.

Screened rooms

The requirement is to screen a room in which a sensitive measurement is being performed from external interference, or to accommodate apparatus which radiate interference in a screened room to keep the surroundings free from interference. The basic method is to use cages of wire mesh, or metal sheet. Both electric and magnetic field components must be considered. Units used for effectiveness are the decibel :

$$s = 20\log\left(\frac{E, B_{noscreen}}{E, B_{withscreen}}\right)$$

and the Napier

$$s = \ln\left(\frac{E, B_{noscreen}}{E, B_{withscreen}}\right)$$

The wire mesh works to screen electric fields because the external flux lines mainly end on the mesh. The effectiveness depends primarily on the size and type of the mesh. Magnetic screening is effected by induced currents; DC magnetic fields are not screened, and low frequency AC magnetic fields are only poorly screened by non magnetic materials. With increasing frequency the magnetic shielding improves and approaches a finite value. Double screens, insulated from each other except at one point, improve the screening. These rooms work well to 20 MHz. Above this the screen room size can equal the cage dimension, causing resonances.

Sheet metal rooms have better screening properties than double walled wire mesh, but breathing is a problem. The screening against electric fields is ideal since no flux can penetrate. The screening of the magnetic component improves with increasing frequency due to the skin effect.

Honeycomb inserts are also used. The grids are wave guides (with the frequencies considered below cut-off), the screening effectiveness of which depends on the ratio of depth to width of the honeycomb up to cm wavelengths. They are used for 100 kHz < f < 1000 MHz.

Misaligned sensor coils

Typical tokamak requirements include the measurement of poloidal fields in the presence of a much larger toroidal field. A small misalignment of the coil will then introduce unwanted field components. There are a number of solution to overcoming this problem

a) subtract data obtained with only the (unwanted) field component by energizing only the offending windings

b) make use of the differential nature of a pick-up coil signal. For example, consider the toroidal field to be the offending field, so that the pick-up coil measures $\frac{dB}{dt} = \frac{dB_{poloidal}}{dt} + \frac{dB_{toroidal}}{dt}$. If the toroidal field is almost steady state (d/dt ≈ 0) during the times of interest, then the differential signal during this time is approximately that required (i.e. from the poloidal field component only). Therefore the temporal integration should be started as late as possible.

PLASMA CURRENT (The Rogowski coil)

The transient plasma current generates a voltage ε in a coil of uniform winding density of n turns per unit length and area A:

$$\varepsilon = n_A A \mu_0 \frac{dI}{dt}$$

from which I_p is deduced after signal integration.

Note a center return should be used to avoid unwanted induced voltages from for example a changing toroidal field.

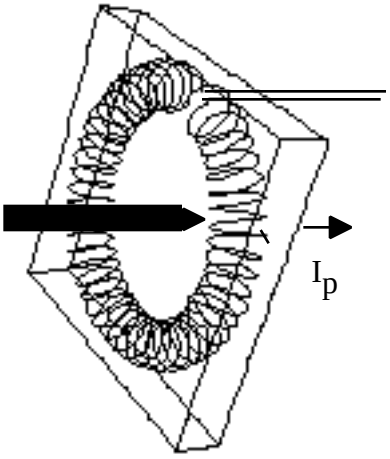

Figure 2a. A Rogowski coil

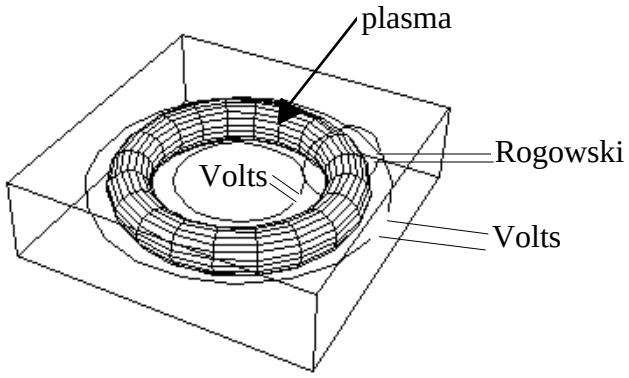

Figure 2b. Coil placement

LOOP VOLTS, VOLTS PER TURN, SURFACE VOLTS

Measure $\varepsilon = 2\pi R E_\varphi = d\Psi/dt$ around the plasma on contour l (e.g. vessel). Poynting's theorem for the poloidal fields alone: $\nabla \times \mathbf{B} = \mu \mathbf{j}$, $\nabla \times \mathbf{E} = -\frac{\partial \mathbf{B}}{\partial t}$, multiplying these by -**E** and **B**/μ, add, and write poloidal component:

$$\frac{\partial}{\partial t}\left(\frac{B_p^2}{2\mu_0}\right) + \nabla \cdot \left(\mathbf{E} \times \frac{\mathbf{B}_p}{\mu_0}\right) + j_\varphi E_\varphi = 0$$

Integrating over the volume V defined by rotating the contour l around φ:

$$\frac{\partial}{\partial t}\left(\frac{L_i I_p^2}{2}\right) + \int_V j_\varphi E_\varphi dV = \oint_l \varepsilon B_\tau \, dl$$

(using $\int_V \nabla \cdot \left(\mathbf{E} \times \mathbf{B}_p\right) dV = \int_S \left(\mathbf{E}_\varphi \times \mathbf{B}_p\right) \cdot d\mathbf{S}_\varphi = \int_S 2\pi R E_\varphi B_p dl$)

L_i is defined by $(L_i I_p^2)/2 = \int (B_p^2/(2\mu_0)) dV$, i.e. $L_i \neq l_i$.

Ohms law $\mathbf{j}\cdot\mathbf{B} = \sigma_{||}\mathbf{E}\cdot\mathbf{B}$, assume $|B_{\varphi 0} - B_\varphi| << B_{\varphi 0}$ so that $E_\varphi = j_\varphi/\sigma_{||}$, gives

$$\frac{\partial}{\partial t}\left(\frac{L_i I_p^2}{2}\right) + \int_V \frac{j_\varphi^2}{\sigma_{||}} dV = I_p \langle \varepsilon \rangle$$

$$\langle \varepsilon \rangle = \frac{1}{\mu_0 I_p} \oint_l \varepsilon B_\tau \, dl$$

For example, suppose the contour is a circle of radius a_l, and

$$\varepsilon = \varepsilon_0 \left[1 + \sum_n \varepsilon_n \cos(n\omega)\right]$$

$$B_t = \frac{\mu_0 I_p}{2\pi a_l}\left[1 + \sum_n \lambda_n \cos(n\omega)\right]$$

Then $\langle\varepsilon\rangle = \varepsilon_0\left(1 + \sum_n \lambda_n \varepsilon_n\right)$

L_i for a "straight" circular tokamak, radius a_p and contour radius a_l is

$$L_i \approx \mu_0 R_p \left[\ln\left(\frac{a_l}{a_p}\right) + \frac{l_i}{2}\right]$$

$\mu_0 l_i/(4\pi)$ is the inductance per unit toroidal length inside the plasma.

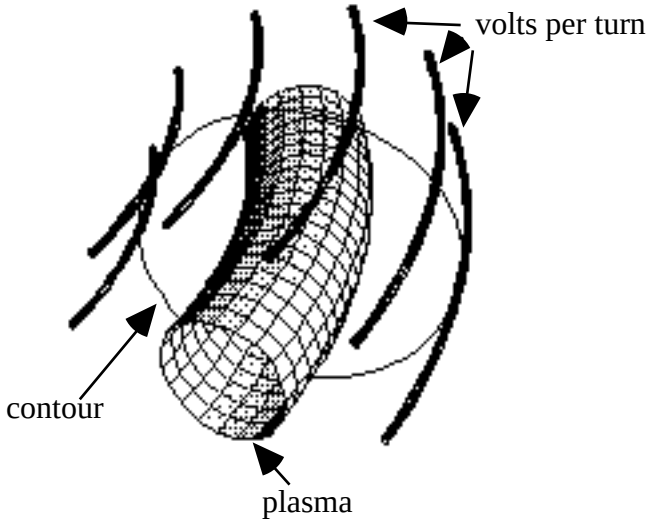

DEDUCTIONS FROM LOOP VOLTS

Average plasma conductivity <σ>:

$$\frac{2\pi R_p I_p^2}{\pi a_p^2 \langle\sigma\rangle} = \int_V \frac{j_\varphi^2}{\sigma_\parallel} dV = I_p \langle\varepsilon\rangle - \frac{\partial}{\partial t}\left(\frac{L_i I_p^2}{2}\right)$$

Conductivity temperature T_σ:

The Spitzer conductivity is

$$\sigma = 1.9 \times 10^4 \frac{T_e^{3/2}}{Z_{eff} \ln(\Lambda_s)}$$

Then T_σ is defined as that temperature which gives a Spitzer conductivity (with Z_{eff} = 1) equal to the average conductivity <σ>.

Average "skin time":

$$\tau_{skin} = \frac{\pi \mu_0 \sigma a_p^2}{16}$$

Energy confinement time τ_E

$$\tau_E = \frac{W}{P_{oh}} = \frac{3\mu_0 \beta_I R_p}{8\Omega_p} = \frac{3\mu_0 \beta_I a_p^2 \langle\sigma\rangle}{16} \quad \frac{\tau_E}{\tau_{skin}} \approx \beta_I$$

CIRCULAR LOW β LARGE R/a EQUILIBRIUM

Use the coordinate system (ρ,ω,−φ) based on a circular contour centered at R_l.

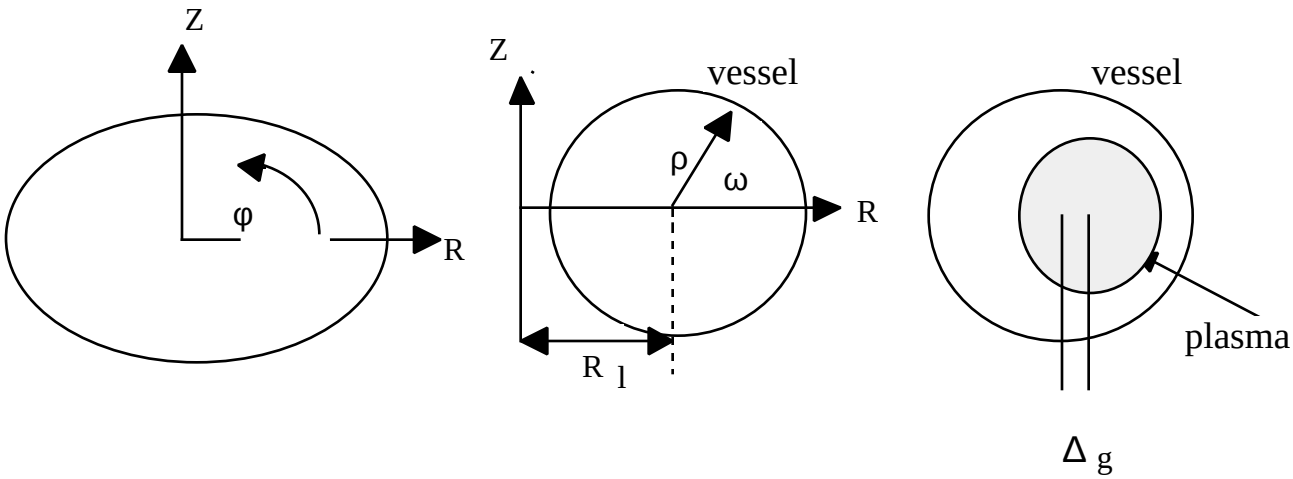

Center of outermost plasma flux surface (the geometric center) is at $R_l+\Delta_g$. For $\rho > a_p$, the plasma minor radius, and taking $\Delta_g/a_p << 1$, we obtain:

$$\frac{\psi}{2\pi} = \frac{\mu_0 R_l I_p}{2\pi}\left[\ln\left(\frac{8R_l}{\rho}\right) - 2\right] - \frac{\mu_0 \rho I_p}{4\pi}\left[1 - \frac{a_p^2}{\rho^2}\left(\Lambda + \frac{1}{2}\right) + \ln\left(\frac{\rho}{a_p}\right) - \frac{2R_l\Delta_g}{\rho^2}\right]\cos(\omega)$$

$$B_\omega(\rho,\omega) = -\frac{\mu_0 I_p}{2\pi\rho} - \frac{\mu_0 I_p}{4\pi R_l}\left[1 + \frac{a_p^2}{\rho^2}\left(\Lambda + \frac{1}{2}\right) + \ln\left(\frac{\rho}{a_p}\right) - 1 + \frac{2R_l\Delta_g}{\rho^2}\right]\cos(\omega)$$

$$B_\rho(\rho,\omega) = -\frac{\mu_0 I_p}{4\pi R_l}\left[1 - \frac{a_p^2}{\rho^2}\left(\Lambda + \frac{1}{2}\right) + \ln\left(\frac{\rho}{a_p}\right) - \frac{2R_l\Delta_g}{\rho^2}\right]\sin(\omega)$$

$$\Lambda = \beta_I + \frac{l_i}{2} - 1$$

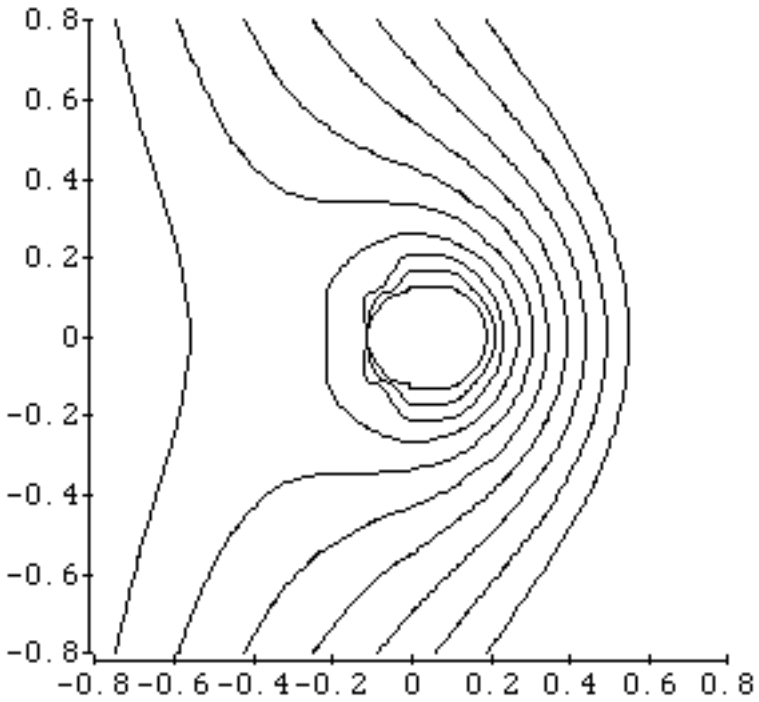

Figure. Flux contours for a (badly drawn) circular plasma with geometric center 0.06 m outside the coordinate center, minor radius 0.265m, $\Lambda = 2$.

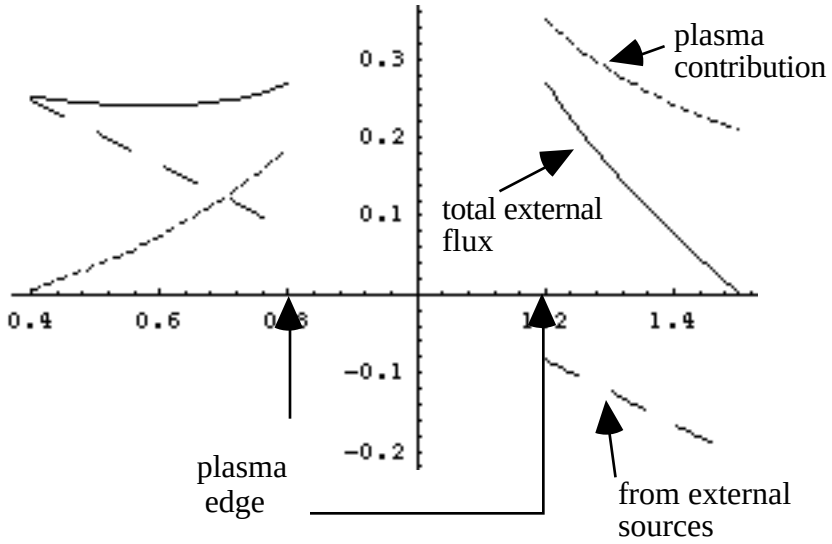

Figure. The external poloidal flux $\psi = \Psi/(2\pi)$ in the plane z = 0 for a plasma with minor radius $a_p = 0.2$m, a major geometric radius $R_g = 1$m, current $I = 1/\mu_0$, and $\Lambda = 2$.

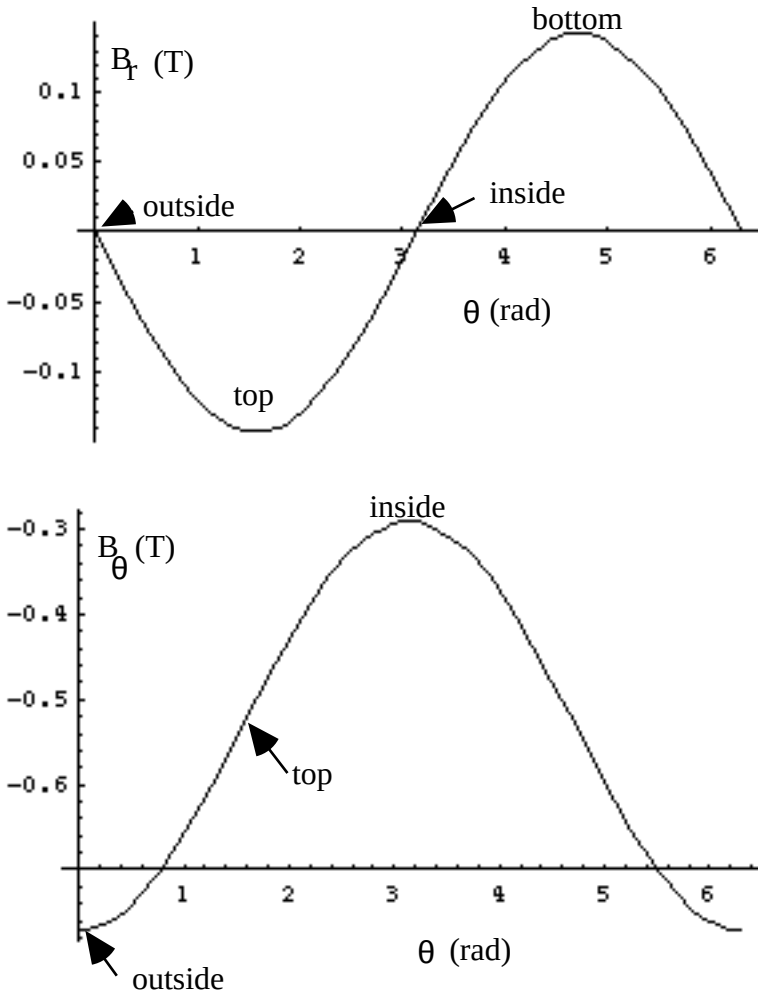

Figure. The field components B_r and B_θ on a contour with minor radius 0.3m placed outside and concentric with the plasma described in previous *Figure.*

POSITION AND $\beta_l + l_i/2$ FOR A CIRCULAR EQUILIBRIUM

B_ω and saddle coils

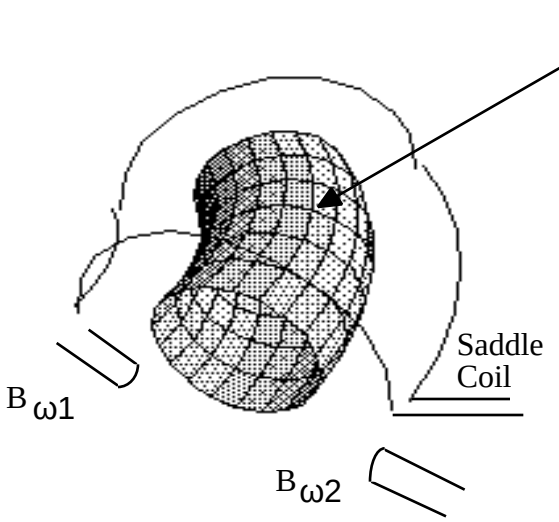

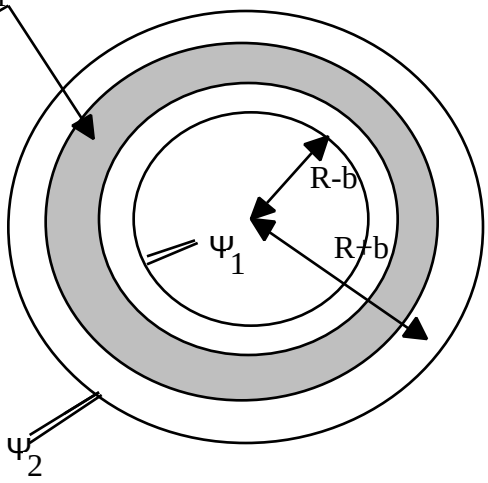

Figure 4a. Saddle and Bω coils Figure 4b. A plan view of poloidal flux loops

$$B = \frac{\Psi_1 - \Psi_2}{4\pi R_l b} = \frac{\psi_1 - \psi_2}{2R_l b}$$

$$\frac{B_{\omega 2} - B_{\omega 1}}{2} + B = \frac{\mu_0 I_p}{2\pi R_l}\left[\ln\left(\frac{b}{a_p}\right) + \beta_l + \frac{l_i}{2} - 1\right]$$

$$\frac{\Delta_g}{b} = \frac{b}{2R_l}\left[\left(\frac{a_p^2}{b^2}\right)\ln\left(\frac{b}{a_p}\right) + 0.5\left(1 - \frac{a_p^2}{b^2}\right)\right]$$

$$+ \frac{\pi b}{\mu_0 I_p}\left[\frac{\left(B_{\omega 2} - B_{\omega 1}\right)}{2}\left(1 - \frac{a_p^2}{b^2}\right) - B\left(1 + \frac{a_p^2}{b^2}\right)\right]$$

Iterate to obtain Δ_g and a_p, and $\Lambda = \beta_I + l_i/2\text{-}1$.

MODIFIED ROGOWSKI AND SADDLE COILS (FIELD CHARACTERIZATION)

We characterize the tangential (subscript τ) and normal (subscript n) fields on a circular contour of radius a_l using a Fourier series:

$$B_\omega = B_\tau = \frac{\mu_0 I}{2\pi a_l}\left[1 + \sum_n \lambda_n \cos(n\omega) + \delta_n \sin(n\omega)\right]$$

$$B_\rho = B_n = \frac{\mu_0 I}{2\pi a_l}\left[\sum_n \kappa_n \cos(n\omega) + \mu_n \sin(n\omega)\right]$$

A modified Rogowski coil (nA cos(ω)) can be used to measure the part of $B_\omega(\rho,\omega)$ proportional to cos(ω), and a saddle coil (width sin(ω)) used to measure that part of $B_\rho(\rho,\omega)$ proportional to sin(ω).

We can measure the components either by performing a Fourier analysis of the data from a set of individual coils measuring $B_n(\omega)$, $B_\tau(\omega)$, or we can construct integral coils which will do the job directly. For example, a "modified Rogowski coil", or "cosine coil", whose winding density (number of turns per unit length) $n_A = n_0\cos(n\omega)$, each turn of area A, will give a signal which, when time integrated, is proportional only to λ_n:

$$\varepsilon = -\frac{d}{dt}\int_S \left(\mathbf{B}\cdot\mathbf{n}_S\, dS\right) = -\frac{d}{dt}\left\{\int_0^{2\pi}\left(B_\omega(\omega) n_A(\omega) a_l A d\omega\right)\right\}$$

$$= -\frac{\mu_0 A n_0}{2\pi}\frac{d}{dt}\left\{I\int_0^{2\pi}\left[\cos(n\omega)\left(1+\sum_n \lambda_n \sin(n\omega)+\mu_n\cos(n\omega)\right)\right]d\omega\right\}$$

$$= -\frac{\mu_0 A n_0}{2}\frac{d}{dt}\{I\lambda_n\}$$

The elemental area $dS = n_A A dl$, the unit length $dl = a_l d\omega$, and n_s is the unit normal to the coil area. That is, the only contribution to the space integral comes from the term $\cos^2(n\omega)$, because $\int_0^{2\pi}\cos(n\omega)\cos(m\omega)d\omega = \pi$ if m = n, otherwise = 0. If the winding density is proportional to $\sin(n\omega)$, the time integrated output is proportional to δ_n. To obtain the coefficients μ_n and κ_n, we must wind a "saddle coil" with n_w turns of width w varying as $\sin(n\omega)$ or $\cos(n\omega)$, so that for a "sin" saddle coil $w(\omega) = w_0\cos(\omega)$, and

$$\varepsilon = -\frac{d}{dt}\left\{\int\left(B(\omega) n_w w(\omega) a_l d\omega\right)\right\}$$

$$= -\frac{\mu_0 w_0 n_w}{2}\frac{d}{dt}\{I\mu_n\}$$

In this case the elemental area $dS = n_w w dl = n_w w a_l d\omega$, the time integrated output provides the coefficient μ. *Figure* shows a cosine coil which measures λ_1. Although it is not illustrated, a center return wound inside the Rogowski coil should be used. *Figure* shows an unfolded "sin saddle coil" measuring μ_1. Of course, we cold also use an array of coils placed on a contour, measuring independent B_τ and B_n at different positions (different ω) and construct the required integrals.

From these two coils we can obtain the two unknowns Λ and Δ_g, assuming a_p.

Iterate to obtain Λ, Δ_g and a_p.

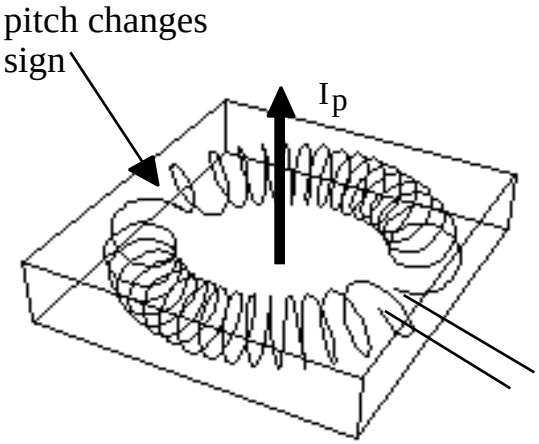

A modified Rogowski coil

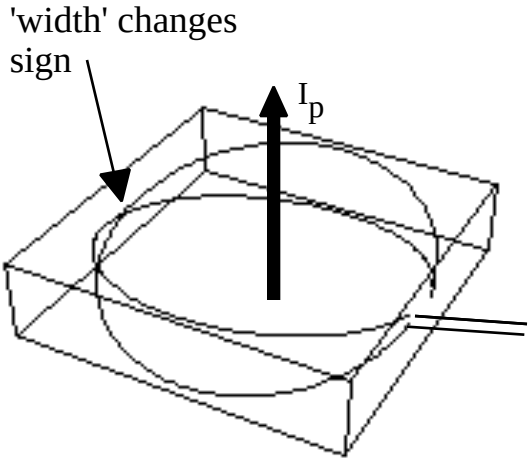

. A saddle coil

MOMENTS OF THE TOROIDAL CURRENT DENSITY

Let fields **q** and g satisfy the equation

$$\frac{1}{\mu}\left(\quad \times \mathbf{q}\right) = \quad \frac{\partial g}{\partial \mu},$$

so that

$$\times\left(\quad \times \mathbf{q}\right) = 0 .$$

Then

$$\int_V \mathbf{q}\cdot \mathbf{j} dV = \int_V \mathbf{q}\cdot\left(\quad \times \frac{\mathbf{B}}{\mu}\right) dV$$

$$= \int_V \left[\cdot \left(\frac{\mathbf{B}}{\mu} \times \mathbf{q}\right) + \frac{\mathbf{B}}{\mu}\cdot\left(\quad \times \mathbf{q}\right)\right] dV$$

$$= \int_V \left[\cdot \left(\frac{\mathbf{B}}{\mu} \times \mathbf{q}\right) + \mathbf{B}\cdot \left(\frac{g}{\mu}\right)\right] dV$$

$$= \int_{S_n} \left[\left(\frac{\mathbf{B}}{\mu} \times \mathbf{q}\right)\cdot \mathbf{n} + \left(\frac{g}{\mu}\right)\mathbf{B}\cdot \mathbf{n}\right] dS_n$$

This has not invoked axisymmetry. Now let **q** = f φ (which has a component only in the f direction, q = f/R) and consider uniform permeability μ_0.

Then we can write an expression for the "multipole moment" Y_m of the toroidal current density

$$Y_m = \frac{1}{I_p}\int_{S_\varphi} f_m j_\varphi dS_\varphi = \frac{1}{\mu_0 I_p}\oint_l \left(f_m B_\tau + R g_m B_n \right) dl$$

where, from

$$\frac{1}{\mu}\left(\nabla \times \mathbf{q} \right) = \frac{1}{\mu}\left(\nabla \times \frac{f}{R}\mathbf{e}_\varphi \right) = \left(\frac{g}{\mu} \right),$$

f_m and g_m are various solutions of

$$\frac{\partial g}{\partial R} = -\frac{1}{R}\frac{\partial f}{\partial z}$$

$$\frac{\partial g}{\partial z} = \frac{1}{R}\frac{\partial f}{\partial R}$$

Remember that $\nabla \times (\nabla \times \mathbf{q}) = 0$, with $\mathbf{q} = f \nabla \varphi = \mathbf{e}_\varphi f/R$, so the equation for f is

$$\frac{\partial^2 f}{\partial R^2} - \frac{1}{R}\frac{\partial f}{\partial R} + \frac{\partial^2 f}{\partial z^2} = 0$$

That is, f is a solution of the homogeneous equilibrium equation and g is a solution of Laplace's equation. Of course, the trick is to find useful expressions for f_m (equivalent to Θ_m) and g_m.

An important point about the method of multipole moments is that the results obtained are sensitive only to currents flowing within the contour l (including vacuum vessel currents if the measurements are made outside this). Thus either the total equilibrium fields, or just the plasma fields, can be used. The plasma fields can be calculated if external conductor currents are known. Using just the plasma fields alone may have advantages in terms of requiring fewer moments to accurately describe the data.

symmetric	asymmetric
$f_0 = 1$	$f_0 = 0$
$g_0 = 0$	$g_0 = -1$
$f_1 = x\left(1 + \frac{x}{2R_c}\right)$	$f_1 = z\left(1 + \frac{x}{R_c}\right)^2$
$g_1 = \frac{z}{R_c}$	$g_1 = -\frac{x}{R_c}\left(1 + \frac{x}{2R_c}\right) + \frac{z^2}{R_c^2}$

Rectangular geometry:

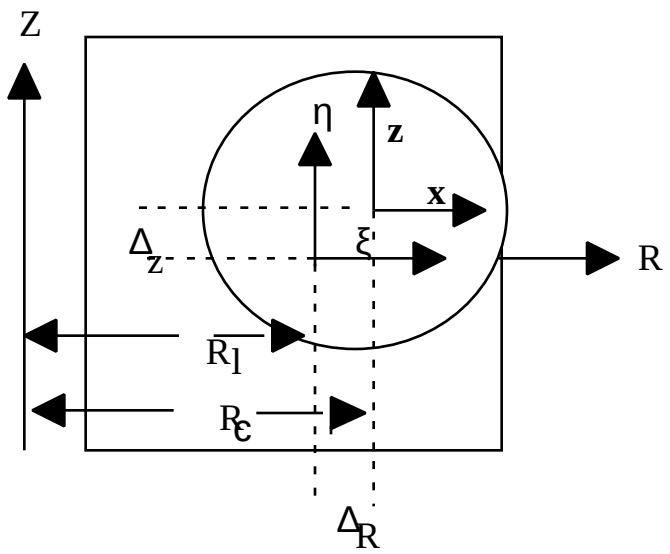

Relate plasma ($\int dS_\varphi$) coordinates to fixed ($\int dl$) coordinates through a plasma displacement Δ_R, Δ_z:

$\xi = x + \Delta_R$, $\eta = z + \Delta_z$, $R_c = R_l + \Delta_R$, $R = R_c + x = R_l + \xi$.

PLASMA POSITION

Define the current center to make $Y_1 = 0$:

$$\oint_l \left[\xi - \Delta_R + \frac{(\xi - \Delta_R)^2}{2R_c} B_\tau + \frac{R_l + \xi}{R_c} \eta B_n\right] dl$$

$$- \oint_l \frac{R_l + \xi}{R_c} \Delta_z B_n dl = 0$$

i.e. the current channel displacement is:

$$\Delta_R = \Delta_{R0} + \Delta_{R1} - \frac{\Delta_{R0}^2}{2R_l}$$

$$\Delta_{R0} = \frac{1}{\mu_0 I_p} \oint_l (\xi B_\tau + \eta B_n) dl$$

$$\Delta_{R1} = \frac{1}{\mu_0 I_p} \oint_l \left[\frac{\xi^2}{2R_l} B_\tau + \frac{\eta\xi}{R_l} B_n\right] dl$$

Therefore the position is measured with a "modified Rogowski coil" whose winding density times cross sectional area varies as $\xi + [\xi^2/(2R_l)]$, and a saddle coil whose width varies as $\eta + [\eta\xi/R_l]$.

Alternatively the integrals can be constructed from discrete local measurements.

Circular geometry ($\xi = a_1 \cos(\omega)$, $\eta = a_1 \sin(\omega)$, neglecting ξ/R_1, then first coil is a "cos Rogowski", second term is a "sin saddle". i.e. position given by Fourier components

$$\Delta_R \approx \frac{a_1}{2}(\lambda_1 + \mu_1) +$$

$$\frac{a_1^2}{4R_1}\left(1 + \frac{\lambda_2}{2} + \mu_2\right) - \frac{a_1^2}{8R_1}(\lambda_1 + \mu_1)^2$$

PLASMA SHAPE

Using higher order moments we can obtain information on the plasma shape. For example, Y_2 determines ellipticity and Y_3 determines triangularity.

That is, with the Rogowski coil measuring I_p and either modified Rogowski and saddle coils, or single point measurements of B_n and B_τ suitably combined, we can construct Y_2.

If we want to use modified Rogowski and saddle coils, then to obtain I_p, Δ_R and Y_2 takes a total of 5 coils.

For a circular contour, and ignoring toroidal effects,

$$Y_2 = -\Delta_R^2 + \Delta_z^2 + \frac{a^2}{2}(\lambda_2 + \mu_2)$$

To interpret the moments it is necessary to assume a plasma current distribution; because the moment is an integral of the current density over the surface S_φ, there is no unique solution for the boundary shape. e.g., consider a uniform current density and a surface described by an ellipse with minor and major half width and half height a and b. Then

$$Y_2 \approx -\frac{ka^2}{2}$$

$\beta_I + l_i/2$

Other integral relationships including the constraint of equilibrium have been obtained:

$$\beta_I + \frac{L_p}{2} = \frac{s_1}{2} + s_2$$

$$s_1 = \frac{2\pi}{\mu_0^2 R_{ch} I_p^2} \int_l \left[\left(B_\tau^2 - B_n^2 \right) \rho \mathbf{n} \cdot \mathbf{e}_\rho - 2 B_\tau B_n \rho \tau \cdot \mathbf{e}_\rho \right] R dl$$

$$s_2 = \frac{2\pi}{\mu_0^2 I_p^2} \int_l \left[\left(B_\tau^2 - B_n^2 \right) \mathbf{n} \cdot \mathbf{e}_\varsigma - 2 B_\tau B_n \tau \cdot \mathbf{e}_\varsigma \right] R dl$$

$\rho = [(R-R_l)^2+z^2]^{1/2}$ is distance from R_l to the contour, $\xi = R - R_l$.

If contour is plasma surface (see 'fast reconstruction') then $L_i = l_i$, $B_n = 0$, and equations for s_1 and s_2 are simplified.

$s_1 = 1$ for a circular discharge.

Because relationships involve squares of fields, we cannot design modified Rogowski and saddle coils to make the measurements. Instead we measure B_n and B_τ at discrete points along the contour, and then construct the required integrals. For circular plasma inside circular contour,

$$\beta_I + \frac{L_p}{2} = 1 + \frac{R_l}{a_l} \left(\lambda_1 + \mu_1 \right)$$

SEPARATION OF β_l AND l_i

For non circular plasmas there is another integral relationship, which provides the parameter $\int_V(2p+B_z^2/\mu_0)dV$ in terms of a measurable contour integral. If the volume averages $<B_z^2>$ and $<B_p2>$ are different, as is the case for non circular discharges, then this measurement allows the required separation.

For near circular plasmas, we must estimate L_i separately. For example, for the simple circular low beta equilibrium we can take a model current distribution

$$j\varphi 0(r) = j_0(1-(r/a)^2)^\alpha$$

Then $l_i = L_i-\ln(a_l/a_p)$, with l_i given as a function of $\alpha = (q_a/q_0 -1)$. By assuming $q_0 = 1$ we can then estimate l_i, and make the separation.

Or we can make a diamagnetic measurement.

DIAMAGNETISM

During formation inside a magnetic field the plasma particles acquire a magnetic moment m:

$$m = Area_{orbit} I_{orbit} = \pi \left(\frac{v}{\omega}\right)^2 \left(\frac{q\omega}{2\pi}\right)$$

Since $\omega = qB/m_e$, we have

$$m = \frac{m_e v^2}{2B}$$

adding up to a total magnetic moment

$$M = nmS_\varphi$$

per unit length of column with cross section S_φ and a number density of n Supposing cylindrical geometry the elementary currents cancel within the homogeneous column, leaving only an azimuthal surface "magnetization' current density j_S:

$$j_S = nm = \frac{nk_bT}{B} = \frac{p}{B}$$

where $p = nk_b(T_e + T_i)$, k_b is Boltzmann's constant. The toroidal field will be modified.

The associated flux from this surface current can be calculated:

$$\Delta\Phi = \pi a_p^2 \Delta B_\varphi = \pi a_p^2 \frac{\mu_0}{2\pi R} I = \pi a_p^2 \frac{\mu_0}{2\pi R} 2\pi R j_S$$

$$= \pi a_p^2 \frac{\mu_0}{2\pi R} 2\pi R \frac{p}{B_\varphi} = \pi a_p^2 \mu_0 \frac{p}{B_\varphi}$$

Using the definition of β_I, we then have

$$\Delta\Phi = \frac{\mu_0^2 I_p^2 \beta_I}{8\pi B_\varphi}$$

Macroscopic picture

Let us consider a toroidal device with no toroidal current plasma current, i.e. a stellarator, in which the necessary rotational transform is produced only by external conductors. Starting with the radial pressure balance, with p = 0 at the plasma edge, and approximating the torus by a long cylinder, then

$$\frac{dp}{dr} = j_\theta B_\varphi$$

integrating over the minor radius (r = 0 to a_p) gives

$$p = -B_\varphi \int_r^{a_p} j_\theta(r')\,dr'$$

and

$$\langle p \rangle = \frac{1}{\pi a_p^2}\int_0^{a_p} 2\pi p\, r\,dr = -\frac{B_\varphi}{\pi a_p^2}\int_0^{a_p} 2\pi r\,dr \int_r^{a_p} j_\theta(r')\,dr'$$

$$= -\frac{B_\varphi}{\pi a_p^2}\int_0^{a_p} \pi r^2 j_\theta(r)\,dr = -B_\varphi \int_0^{a_p} \frac{S(r)}{\pi a_p^2} j_\theta(r)\,dr$$

Then $j_{se} = \int_0^{ap} S(r)/(\pi a_p^2) j_\theta(r)dr$ is the effective surface current density at the plasma edge as a consequence of the finite plasma pressure.

Paramagnetic and diamagnetic flux

Outside the plasma the toroidal field has the form $B_{\varphi e} = B_{\varphi 0}(R_0/R)$, with $B_{\varphi 0}$ the value at a fixed radius R_0. This toroidal field, together with the poloidal field, takes part in balancing the plasma pressure.

We need an equation relating fields to pressure. Substituting $\nabla \times \mathbf{B} = \mu_0 \mathbf{j}$ into $\nabla p = \mathbf{j} \times \mathbf{B}$ yields (using $\mathbf{B} \times (\nabla \times \mathbf{B}) = \frac{\nabla \mathbf{B}^2}{2} - (\mathbf{B} \cdot \nabla)\mathbf{B}$)

$$\nabla \left(p + \frac{B^2}{2\mu_0} \right) = (\mathbf{B} \cdot \nabla) \frac{\mathbf{B}}{\mu_0}$$

For a straight axially symmetric system ($\partial/\partial z = 0$) we obtain

$$\frac{\partial}{\partial r} \left(p + \frac{B_z^2 + B_\theta^2}{2\mu_0} \right) = -\frac{B_\theta^2}{r\mu_0}$$

Multiplying each side by r^2, letting u = r^2, du = 2rdr, dv = ∂/∂r(.), v = (..), we obtain by integrating by parts ($\int$udv = uv - $\int$vdu)

$$r^2\left(p + \frac{B_z^2 + B_\theta^2}{2\mu_0}\right)\Bigg|_0^a - \int_0^a \left(p + \frac{B_z^2 + B_\theta^2}{2\mu_0}\right) 2r\,dr = -\int_0^a \frac{B_\theta^2}{\mu_0} r\,dr$$

i.e.,

$$\left(p + \frac{B_z^2 + B_\theta^2}{2\mu_0}\right)_{r=a} = \frac{1}{\pi a^2}\int_0^a \left(p + \frac{B_z^2}{2\mu_0}\right) 2\pi r\,dr$$

That is, ignoring curvature and equating B_z with B_φ, the pressure balance constraint is

$$2\mu_0\langle p\rangle = B_{\theta a}^2 + B_{\varphi e}^2 - \left\langle B_\varphi^2 \right\rangle$$

where B_φ is the toroidal field inside the plasma, $B_{\varphi e}$ is the toroidal field outside the plasma, and <..> means an average over the plasma radius.

In a tokamak $B_{\varphi e} \sim \langle B_\varphi \rangle$, so that

$$B_{\varphi e}^2 - \left\langle B_\varphi^2 \right\rangle \approx 2B_{\varphi e}\left\langle B_{\varphi e} - B_\varphi \right\rangle = \frac{2B_{\varphi e}\delta\Phi}{\pi a_p^2}$$

where

$$\delta\Phi = \pi a_p^2 \left\langle B_{\varphi e} - B_\varphi \right\rangle$$

Then

$$\beta_I = 1 + \frac{8\pi B_{\varphi e}\delta\Phi}{\mu_0^2 I_p^2}$$

Paramagnetic: $\delta\Phi_p = -\dfrac{\mu_0^2 I_p^2}{8\pi B_{\varphi e}}$

Diamagnetic: $\delta\Phi_d = -\delta\Phi_p \beta_I$

In a torus curvature must be accounted for, corrections with coefficients (a/R) appear. For $\beta_I << R/a$ these corrections are small. For non circular cross sections the generalized pressure moments show that $\beta_I = s_1 + 8\pi B_{\varphi e}\delta\Phi/(\mu_0 I_p)^2$

$\beta_I > 0$ means $dB_\varphi^2/dr > 0$, and $\beta_I < 0$ means $dB_\varphi^2/dr < 0$.

DIAMAGNETIC MEASUREMENT

$\delta\Phi$ ~ 1 mWb, compared to typical vacuum flux Φ_V = 1 Wb enclosed by same loop. Therefore measurements to better than 1 part in 10^4 to get 10% accuracy in values of β_I.

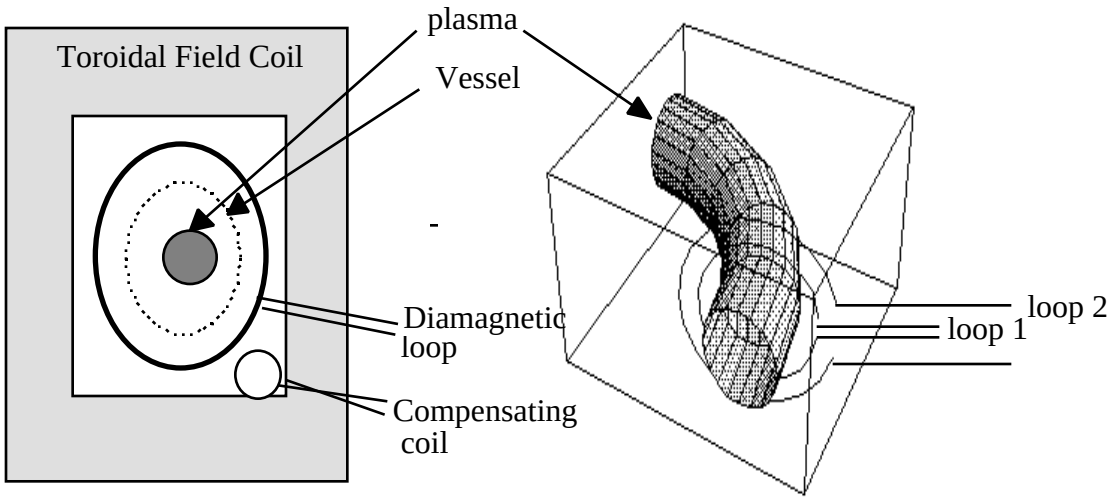

Figure 5a. Diamagnetic loop and compensating coil

Figure 5b. Two concentric diamagnetic loops

Two toroidal flux loops, at different minor radii. The two concentric loops have radii b_1 and b_2, and R_l is the major radius of the loops. Then, with $B_{\varphi e} = B_{\varphi 0} R_l / R$,

$$\Phi(b_i) = 2\pi R_l B_{\varphi 0}\left[R_l - \left(R_l^2 - b_i^2\right)^{\frac{1}{2}}\right] + \delta\Phi$$

$$\delta\Phi = \Phi(b_1) - k\left(\Phi(b_2) - \Phi(b_1)\right);$$

$$k = \frac{b_1^2}{b_2^2 - b_1^2}\,\frac{\sqrt{R_l^2 - b_1^2} + \sqrt{R_l^2 - b_2^2}}{R_l + \sqrt{R_l^2 + b_1^2}}$$

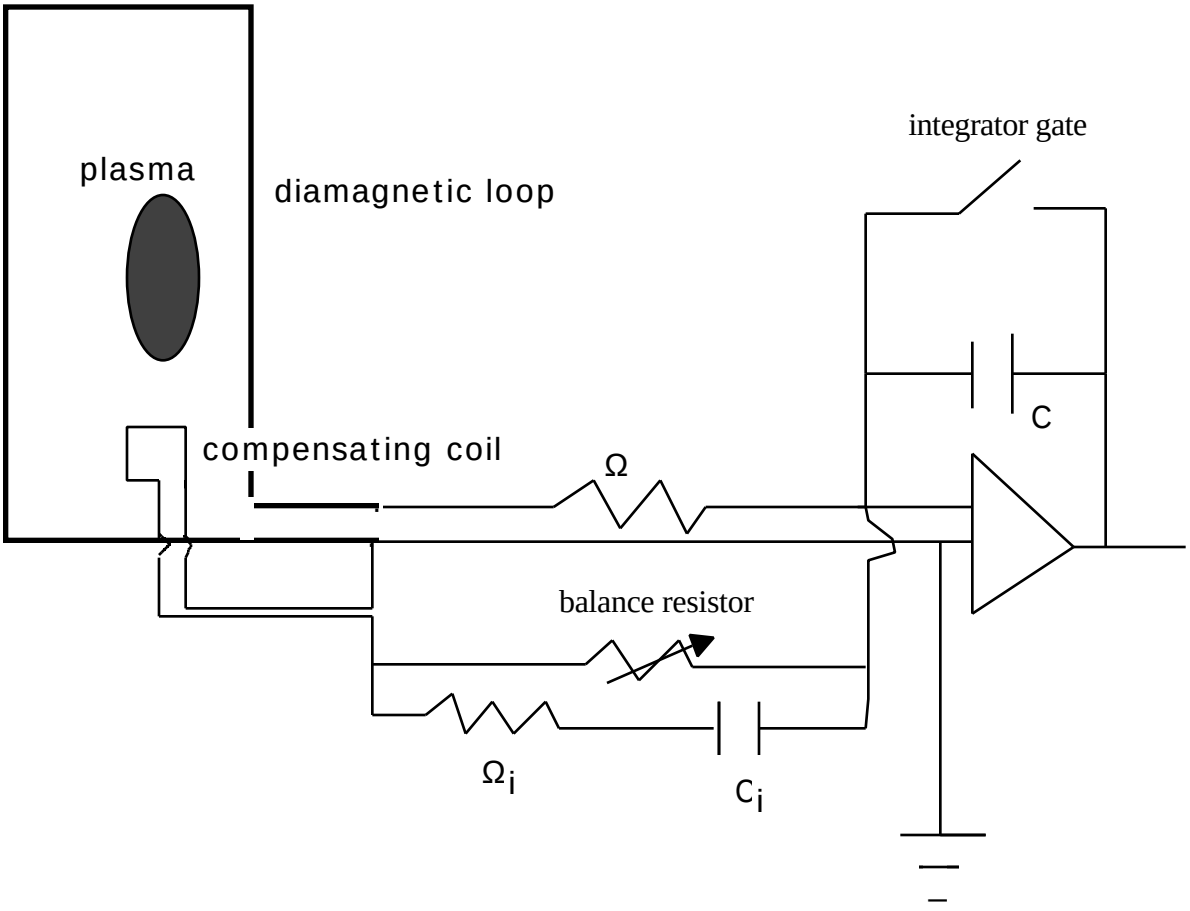

FAST SURFACE RECONSTRUCTION

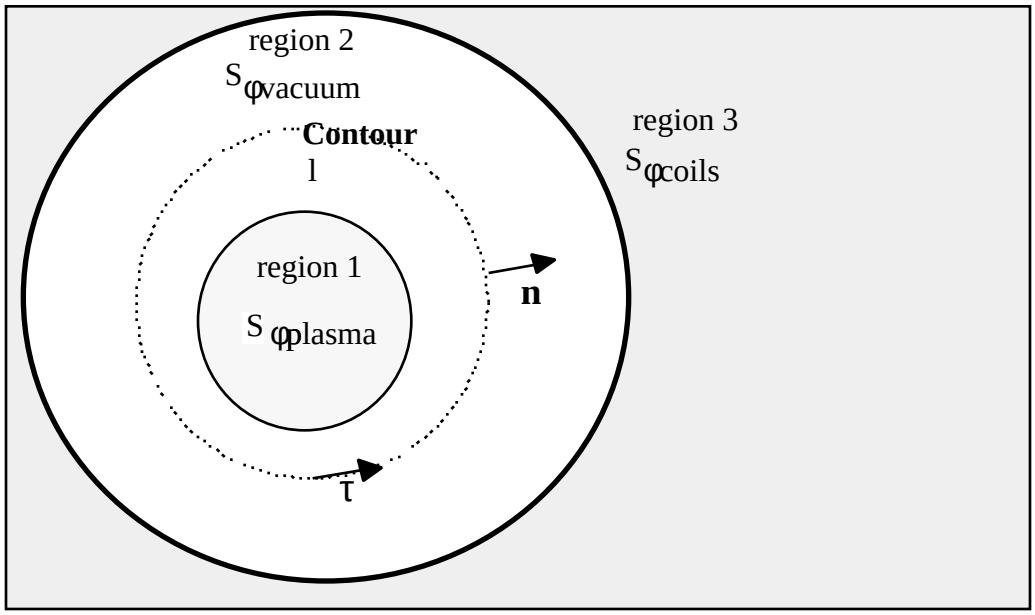

Figure 6. Boundary regions

To find plasma boundary we must know $\psi(R,Z)$ in region 2

a) $\partial\psi/\partial n$ (i.e. B_τ) and either $\partial\psi/\partial\tau$ (i.e. B_n) or ψ on part of l (spec. $\partial\psi/\partial\tau$ is equivalent to spec. ψ to within an unimportant constant after integration). Cauchy condition.

b) currents in region 3, and either $\partial\psi/\partial n$, $\partial\psi/\partial\tau$ or ψ on l.

Usually use an apparently over determined problem, e.g. all currents, $\partial\psi/\partial n$ and $\partial\psi/\partial\tau$ on l. In fact this is not so because we only have the fields at discrete points, and the boundary conditions are applied in a least squares sense.

Various representations for plasma current (hence ψ_{plasma}) have been used. Generally the coefficients in an expansion are altered numerically to provide a minimum "chi squared" between some measured and computed fields or fluxes.

EXAMPLE OF FAST RECONSTRUCTION

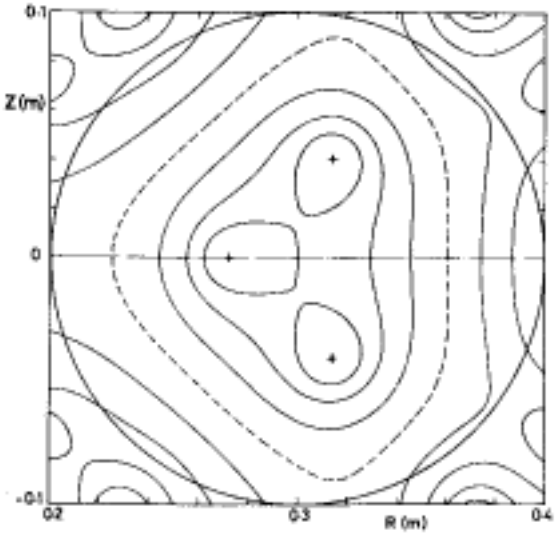

A fast reconstruction (filaments).

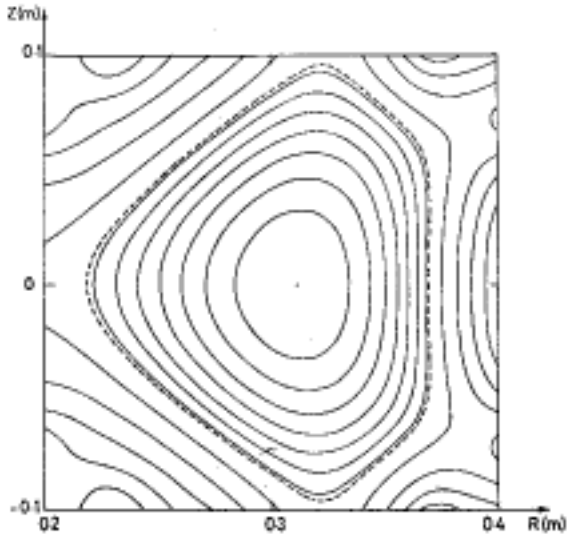

A full reconstruction (equilibrium).

MIRNOV OSCILLATIONS

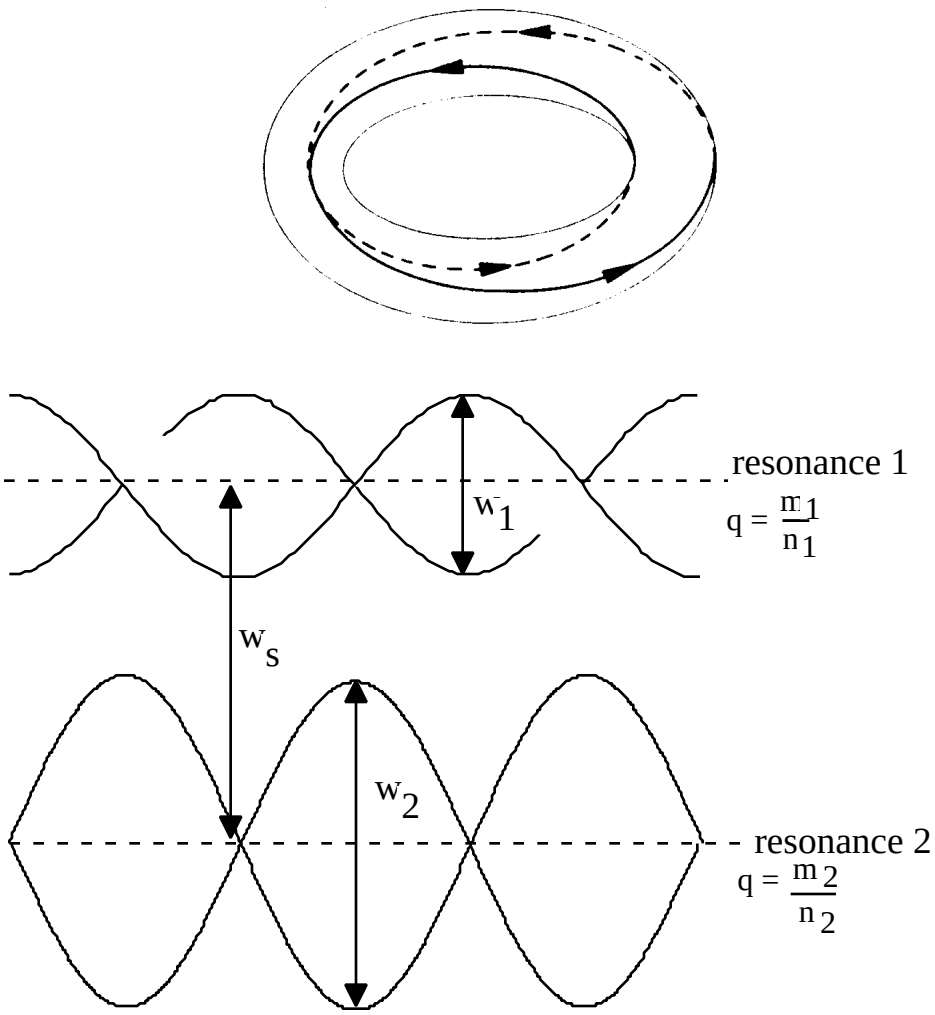

Magnetic islands play a role in determining transport. Their spatial structure is approximately of the form $\exp(i(m\theta+n\varphi))$, and they are located at surfaces where $q = m/n$.

In terms of the Fourier coefficients of the radial component of perturbing field $b_{r,mn}$ at the resonant surface r_{mn} (where q = m/m), the island half width w is given by:

$$w_i = 2\sqrt{\frac{4q^2|b_{rmn}|R}{mB_\varphi \frac{\partial q}{\partial r}}}$$

Mirnov first studied them with b_θ loops, measuring $\partial b_\theta/\partial t$ outside the plasma.

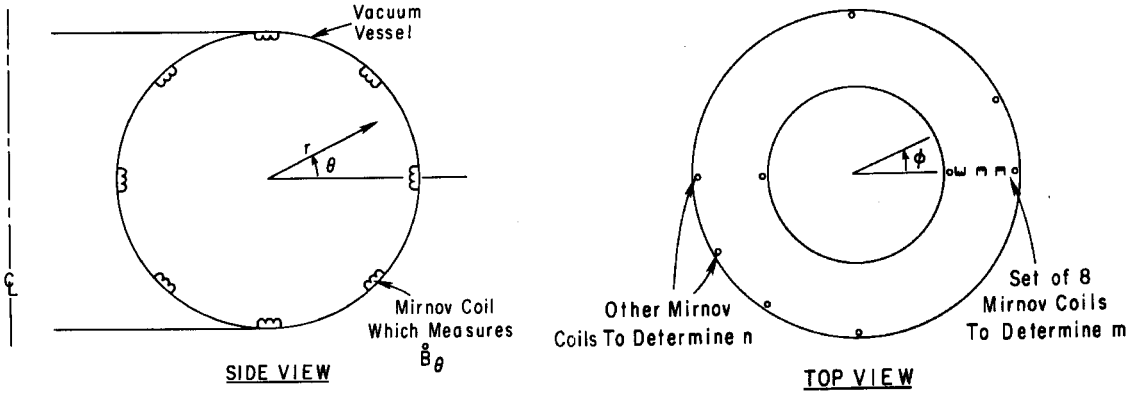

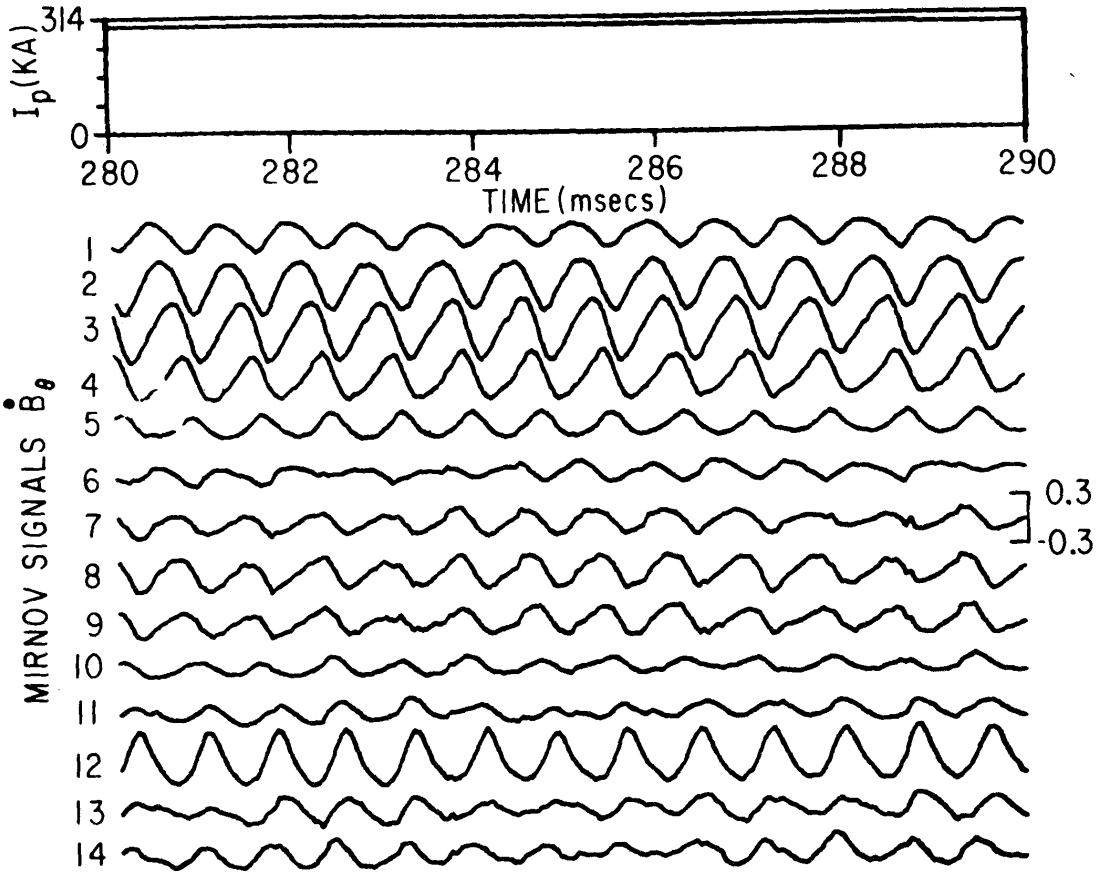

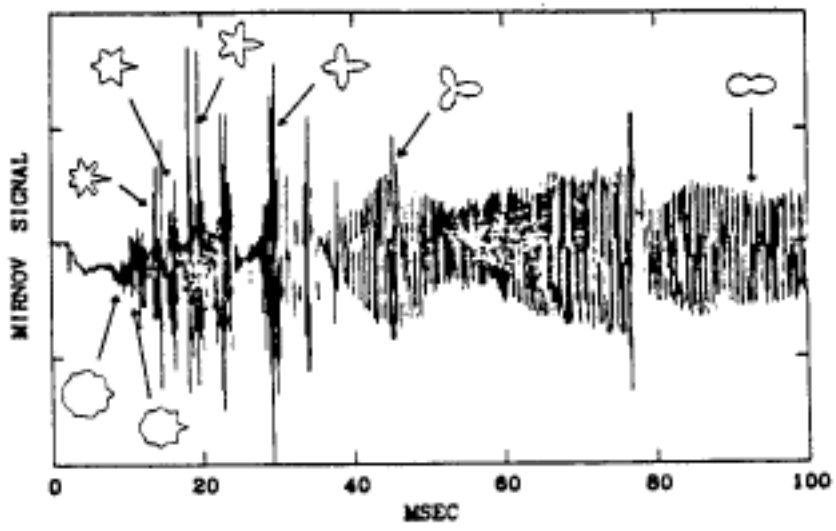

$\partial b_\theta/\partial t$ and polar plots of $b_\theta(\theta)$ during the current rise.

Because the coils are outside the plasma they do not measure the field strength at the integer q surface. To extrapolate the fields (measured at the plasma edge) inwards to the singular surface to allow the island width to be derived we can represent the fluctuations as being caused by current filaments aligned along the field lines.

Complications:

1) Vacuum vessels

2) Toroidal geometry

a) j_{mn} produces stronger field at inner equator,

b) perturbation is displaced because of Shafranov shift

c) the pitch of the field lines is no longer constant. Replace θ by θ^*:

$$\theta^* = \frac{\varphi}{q_{MHD}} = \theta - \frac{a}{R_g}\left(\beta_I + \frac{l_i}{2} + 1\right)\sin(\theta)$$

POLOIDAL MODE STRUCTURE

Fourier transform in θ^* to obtain the amplitude of each component $\cos(m\theta^*+n\varphi-\omega_{mn}t)$.

This has been done both computationally, and using analog multiplexing.

It is important to use the toroidal (θ^*) expressions, otherwise incorrect m values are inferred.

Another technique is to look in the frequency domain . With coils placed both poloidally and toroidally around the plasma, the relationship between the signal phases identifies m and n without the amplitudes being known. In the frequency domain we can reject noise, and other modes at frequencies other than ω_{mn}. Again the toroidal expressions must be used.

INTERNAL PLASMA MEASUREMENTS

So far we have been concerned with measurements of fields taken outside the plasma. In comparatively low temperature plasmas (say T_e < 50 to 100 eV), we can design pickup coils to make internal measurements. There is always the worry that the insertion of such a coil changes the very plasma characteristics we would like to determine. This fear is usually allayed by monitoring certain characteristic plasma features (sawtooth activity, Mirnov activity, loop voltage) to make sure they do not change significantly during probe insertion. *Figures* show a possible coil set up which might be used. The coil itself must be protected from the plasma, typically by a stainless steel case, possibly surrounded by a carbon shield. The geometry of the surrounding materials must be carefully chosen if we are looking at high frequencies so as not to cut off the very signals we want to measure.

. Typical internal magnetic probe construction

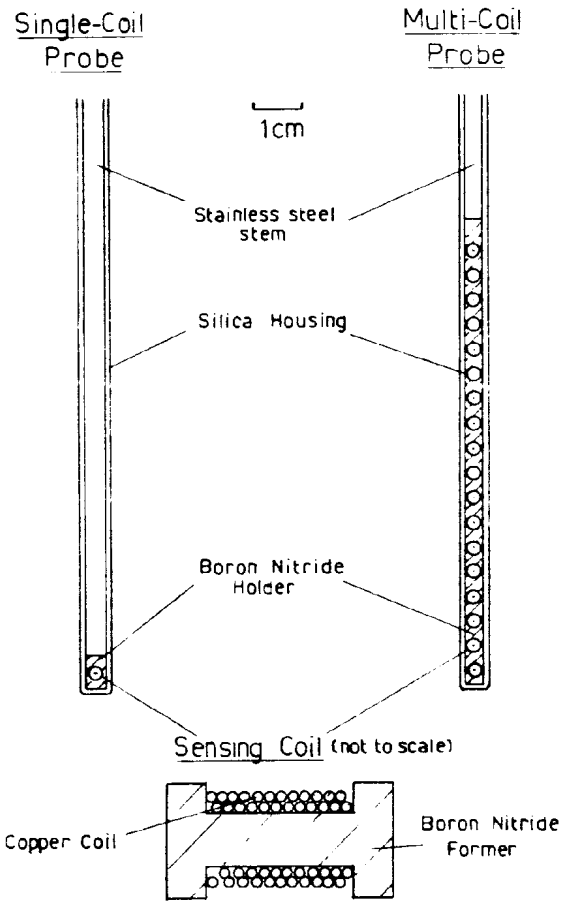

. Typical probe insertion geometry.

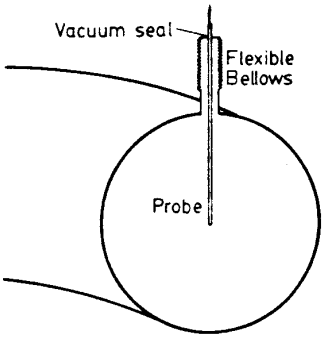

Equilibrium

We first discuss the equilibrium. From the basic field measurements themselves we can, assuming circular straight geometry, reconstruct the current from the equations

$$j_\varphi = \frac{1}{\mu_0 r}\frac{d}{dr}\left(rB_\theta\right)$$

$$j_\theta = -\frac{1}{\mu_0}\frac{d}{dr}\left(B_\varphi\right)$$

i.e. to obtain $j_\varphi(r)$ we only need the radial dependence of B_θ. Unfortunately we have to contend with non circularity and toroidicity. One technique which has been applied is illustrated by the results shown in *Figure* where small pick-up coils were used to measure the poloidal magnetic field at current peak in a small tokamak (TNT in Japan).

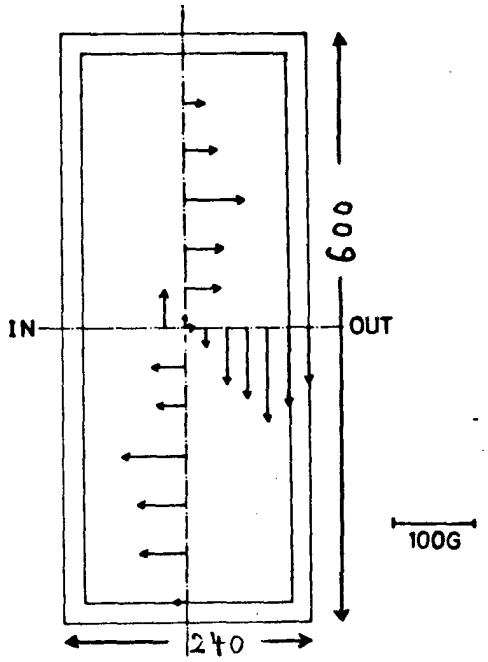

The measured poloidal magnetic field at the current peak (700 μsec). The dimensions are in millimeters.

Equilibrium poloidal fields measured in TNT

The radial component $B_R(R_0,z)$ is measured along a vertical line $R = R_0$, and the vertical component $B_Z(R,0)$ is measured along a line $z = 0$. The results are fitted to expressions of the form

$$B_R(R_0,z) = \sum_{n=0}^{N} a_n z^n$$

$$B_Z(R,0) = \sum_{n=0}^{N} b_n R^n$$

The magnetic axis is found where from the zero crossing of the resulting polynomials. The flux function is found by integration:

$$\psi\left(R_0, z\right) = -R_0 \int \sum_{n=0}^{N} \left(a_n z^n\right) dz + const$$

$$\psi\left(R\ , 0\right) = \int \sum_{n=0}^{N} \left(b_n R^{n+1}\right) dR + const$$

The current density is then obtained as

$$\mu_0 j = \frac{\partial B_R}{\partial z} - \frac{\partial B_z}{\partial R}$$

The constants (giving $\partial B_R/\partial z$ at z = 0 and $\partial B_Z/\partial R$ at R = R_0) must be determined by making some assumptions concerning the plasma shape, say that it is mostly elliptic. Some examples of the results of this analysis, where N = 5, are shown in *Figure* for the fluxes and *Figure* for the current density.

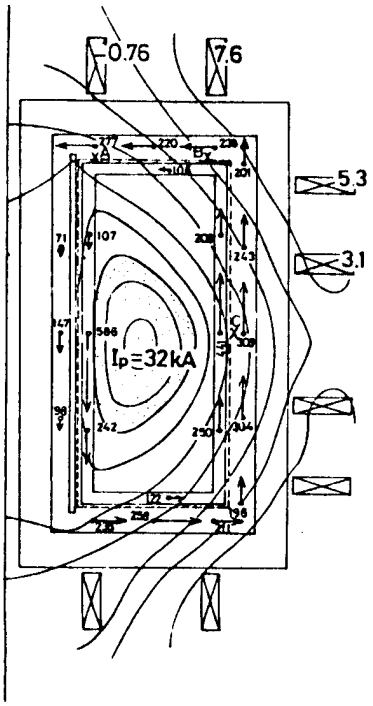

A rough sketch of magnetic surface at the current maximum. The equi-psi surfaces are drawn for every $\pi \times 10^{-3}$ V·sec. Numbers at arrows show the field component parallel to the arrows in unit of gauss. The shaping coil current is presented in kAt, and minus sign means that the coil current is parallel to the plasma current. Coil current has up-to-down symmetry.

Flux surfaces reconstructed for TNT.

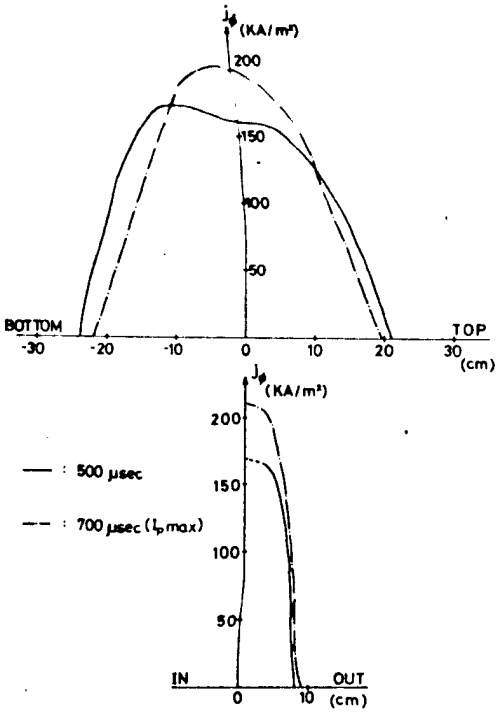

A typical example of the current density profile at the current rising stage (t = 500 μsec) and at the current peak (t = 700 μsec). Origins of the graphs correspond to the center of the vacuum vessel.

Current density profiles for TNT

Internal electric field

Internal magnetic measurements are also used to determine the internal electric field. From Faraday's law

$$\oint_l \mathbf{E}\cdot\mathbf{dl} = -\frac{d}{dt}\left(\int_S \mathbf{B}\cdot\mathbf{n}\,dS\right)$$

we have, applying this to the geometry of *Figure*

$$E_\varphi(r) = E_\varphi(a) - \int_r^a \frac{d}{dt} B_\theta\, dr$$

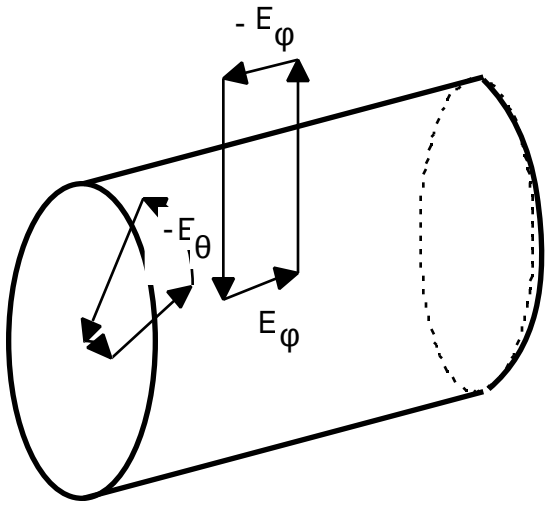

The geometry used to describe the measurements of internal electric field

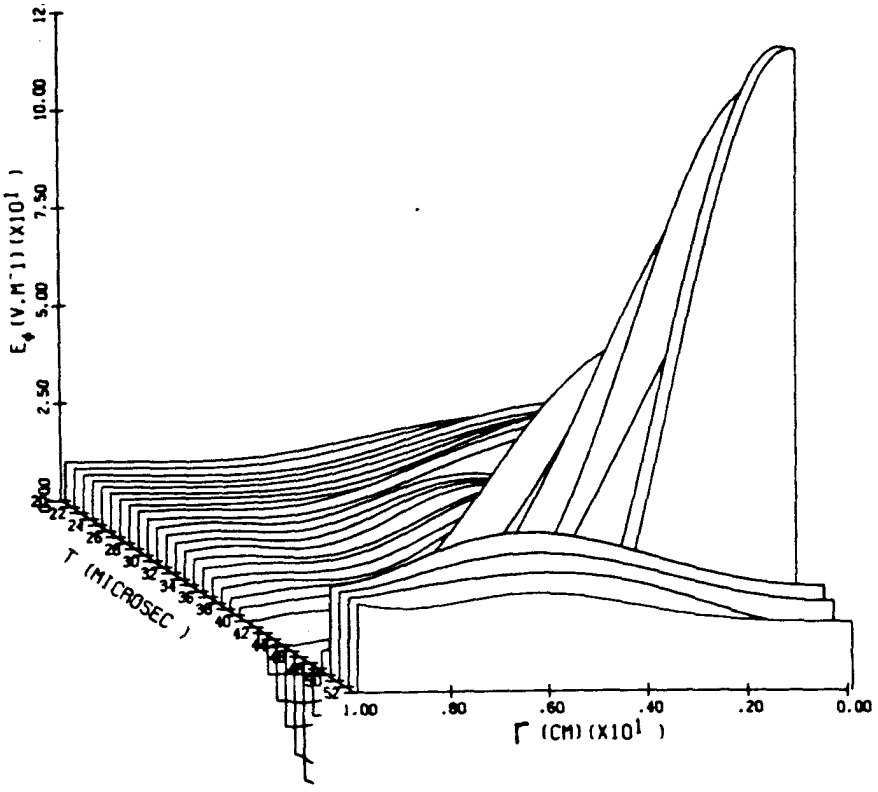

The internal electric field prior to a disruption
(from Hutchinson)

Figure shows some spatial profiles of E_φ from this analysis just before and at a disruption. Although the edge electric field goes negative (the negative voltage spike) the internal electric field strongly positive. In principle, having measured j and E we could derive the local conductivity.

Mirnov Oscillations

The same probes used to measure the internal equilibrium properties can be used to look at the Mirnov fluctuations (as long as the coils have a sufficiently high frequency response). Data from such experiments has isolated the radial dependence of the fluctuating b_r, $b\theta$ fields, as shown in *Figure* It agrees with our discussion in previous section, namely b $(r_{mn}/r)^{m+1}$ for r > rmn without a vacuum vessel. In the presence of a conducting vessel at r = r_W we must account for the image currents which flow, so for example we would expect

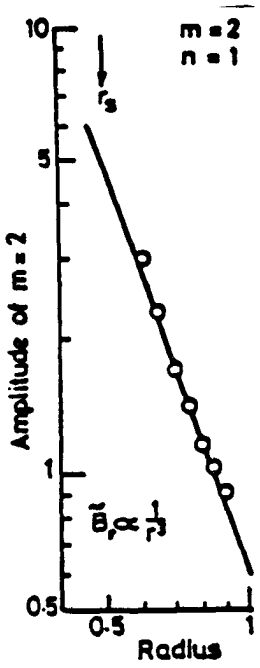

Radial dependance of m=2/n=1

The measured radial dependence of the fluctuating poloidal fields (Mirnov oscillations) from and m = 2 tearing mode (measurements in TOSCA).